*Inorg. Chem.* **2005**, *44*, 2719–2727

# Five New Zinc Phosphite Structures: Tertiary Building Blocks in the Construction of Hybrid Materials

**Jian Fan,[†] Carla Slebodnick,[†] Diego Troya,[†] Ross Angel,[‡] and Brian E. Hanson*,[†]**

*Department of Chemistry, Virginia Polytechnic Institute and State University, Blacksburg, Virginia 24061, and Department of Geosciences, Virginia Polytechnic Institute and State University, Blacksburg, Virginia 24061*

Received December 20, 2004

The syntheses and structures of five new zinc phosphites $[Zn(HPO_3)(C_4H_6N_2)]$ (**1**), $[Zn_2(HPO_3)_2(C_{10}H_{10}N_2)_2]_2$ (**2**), $[Zn(HPO_3)(C_{14}H_{14}N_4)_{0.5}]$ (**3**), $[Zn_2(HPO_3)_2(C_{14}H_{14}N_4)]\cdot 0.4H_2O$ (**4**), and $[Zn_2(HPO_3)_2(C_{14}H_{14}N_4)]$ (**5**) are reported. In compounds **1**–**3**, the zinc atoms are ligated by 1-methylimidazole, 1-benzylimidazole, and 1,4-bis(imidazol-1-ylmethyl)-benzene, respectively, while compounds **4** and **5** are synthesized in the presence of the same bifunctional ligand, 1,3-bis(imidazol-1-ylmethyl)benzene. The inorganic framework of compound **1** is composed of vertex-shared $ZnO_3N$ and $HPO_3$ tetrahedra that form 4-rings, which, in turn, are linked to generate a one-dimensional ladder structure. In **2**, the inorganic framework is composed of 4-rings and 8-rings to form the well-known $4.8^2$ 2D network. This is connected via C–H$\cdots\pi$ interactions between 1-benzylimidazole ligand to generate a pseudo-pillared-layer structure. In **3**, the inorganic framework again has the $4.8^2$ topology pillared by the bis(imidazole) ligand, 1,3-bis(imidazol-1-ylmethyl)benzene. In **4**, a new layer pattern is observed. Specifically, three edge-sharing 4-rings form triple-fused 4-rings. These tertiary building units are further connected to form 12-rings. The alternating triple 4-rings and 12-rings form a previously unknown 2D inorganic sheet. The sheets are joined together by the bis(imidazole) ligand, 1,3-bis(imidazol-1-ylmethyl)benzene, to generate a 3D pillared-layer structure. In **4**, benzene rings and imidazole rings stack in a zigzag pattern in the interlayer space. A significant role for the triple 4-ring tertiary building unit in the formation of hybrid inorganic/organic metal phosphite structures is proposed for **4** and **5**. In **5**, the triple 4-rings fuse to give a 1D stair-step structure. Calculations show that the triple 4-ring pattern observed in the linear ladder structure of **1** is more stable than that in the stair step pattern of **5**.

## Introduction

The concept of secondary building units, SBUs, in the construction of hybrid inorganic/organic zinc phosphates and zinc phosphites is critical to the understanding of structure of these materials.[1] The primary building units, PBUs, namely zinc and phosphorus tetrahedra, may be linked in a remarkable variety of patterns. One common motif is the zinc phosphate/phosphite 4-ring, which is recognized as a secondary building unit or SBU.[2−7] These building blocks are depicted in Scheme 1. Isolated 6-rings may also be considered as an SBU in the formation of $6^3$ nets,[8] and other SBUs are possible. The formation of the 4-ring SBU under hydrothermal conditions is implied by the many observed structures that have this motif. Common themes include

* Author to whom correspondence should be addressed. E-mail: hanson@vt.edu.

[†] Department of Chemistry.

[‡] Department of Geosciences.

(1) (a) Rao, C. N. R.; Natarajan, S.; Choudhury, A.; Neeraj, S.; Ayi, A. A. *Acc. Chem. Res.* **2001**, *34*, 80. (b) Cheetham, A. K.; Férey. G.; Loiseau, T. *Angew. Chem., Int. Ed*. **1999**, *38*, 3268. (c) Murugavel. R.; Walawalkar, Dan, M.; Roesky, H. W.; Rao, C. N. R. *Acc. Chem. Res.* **2004**, *37*, 763. (d) Johnstone, J. A.; Harrison, W. T. A. *Inorg. Chem*. **2004**, *43*, 4567.

(2) (a) Rao, C. N. R.; Natarajan, S.; Neeraj, S. *J. Am. Chem. Soc*. **2000**, *122*, 2810. (b) Natarajan, S.; Wullen, L. V.; Klein, W.; Jansen, M. *Inorg. Chem*. **2003**, *42*, 6265. (c) Lin, Z.-E.; Zhang, J.; Zheng, S.-T.; Yang, G.-Y. *Inorg. Chem. Chem*. **2003**, *6*, 1035. (d) Harrison, W. T. A.; Hanooman, L. *J. Solid State Chem*. **1997**, *131*, 363. (e) Dan, M.; Udayakumar, D.; Rao. C. N. R. *Chem. Commun*. **2003**, 2212. (f) Harrison, W. T. A.; Yeates, R. M.; Phillips, M. L. F.; Nenoff, T. M. *Inorg. Chem.* **2003**, *42*, 1493. (g) Lin, Z.-E.; Zhang, J.; Zheng, S.-T.; Wei, Q.-H.; Yang, G.-Y. *Solid State Sci*. **2003**, *5*, 1435. (h) Neeraj, S.; Natarajan, S.; Rao, C. N. R. *J. Solid. State Chem*. **2000**, *150*, 417.

(3) (a) Gordon, L. E.; Harrison, W. T. A. *Inorg. Chem.* **2004**, *43*, 1808. (b) Chavaz, A. V.; Nenoff, T. M.; Hanooman, L.; Harrison, W. T. A. *J. Solid State Chem*. **1999**, *147*, 584. (c) Rao, C. N. R.; Natarajan, S.; Neeraj, S. *J. Am. Chem. Soc*. **2000**, *122*, 2810. (d) Ayi, A. A.; Neeraj, S.; Choudhury, A.; Natarajan, S.; Rao. C. N. R. *J. Phys. Chem. Solids* **2001**, *62*, 1481. (e) Reinert, P.; Zabukovec, N.; Patarin, J.; Kaucic, V. *Eur. J. Solid State Inorg. Chem*. **1998**, *136*, 373.

10.1021/ic048204u CCC: $30.25 
Published on Web 03/23/2005

**Scheme 1.** Drawings of PBUs, SBUs, and TBUs

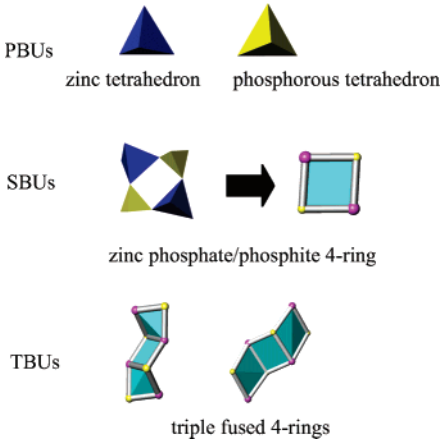


isolated 4-rings in molecular compounds,[2] chains of 4-rings in ladder structures,[3] and sheets of 4-rings linked through corners to make alternating 4- and larger number-ring structures in two dimensions.[4] The SBU concept implies that the 4-rings exist in solution and that the final structure is dictated, in part, by the manner in which these are modified by the added organic template or ligand.[3a,4f,6] Alternatively, the observed structure could form directly from the self-assembly of primary building units or from tertiary building units, TBUs. A building unit may be considered tertiary if it can be derived from two or more SBUs. There is value in identifying tertiary patterns in hybrid inorganic/organic materials as a visualization tool and as a hint to possible synthesis mechanisms. If tertiary patterns can be controlled during synthesis, it may be possible to devise rational syntheses of specific hybrid inorganic/organic structures.[7b] Here, we suggest that the triple-fused 4-ring may be considered as a tertiary building unit in two new zinc phosphite/imidazolyl hybrid compounds. The triple 4-ring has been observed in related structures in the literature.[9]

The construction of higher dimensional structure in zinc phosphate/phosphite may be viewed as the self-assembly of building units, PBUs, SBUs, and TBUs.[6f] The synthesis of hybrid inorganic/organic materials with novel topologies is accomplished with organic ligand to interfere in this aufbau process,[1a] by means of connecting or separating the building units. To date only a few examples of the hybrid inorganic/organic zinc phosphites have been reported.[1d,5f,10] In this work, 1-methylimidazole, 1-benzylimidazole, 1,4-bis(imidazol-1-ylmethyl)benzene, and 1,3-bis(imidazol-1-ylmethyl)benzene are used as ancillary ligands, and five new zinc phosphites $[Zn(HPO_3)(C_4H_6N_2)]$ (**1**), $[Zn_2(HPO_3)_2(C_{10}H_{10}N_2)_2]_2$ (**2**), $[Zn(HPO_3)(C_{14}H_{14}N_4)_{0.5}]$ (**3**), $[Zn_2(HPO_3)_2(C_{14}H_{14}N_4)]\cdot 0.4H_2O$ (**4**), and $[Zn_2(HPO_3)_2(C_{14}H_{14}N_4)]$ (**5**) are synthesized and structurally characterized.

## Experimental Section

**Materials and Measurements.** All commercially available chemicals are of reagent grade and used as received without further purification. The ligands 1,4-bis(imidazol-1-ylmethyl)benzene[11a] and 1,3-bis(imidazol-1-ylmethyl)benzene[11b] were synthesized by the reaction of imidazole with α,α′-dibromo-*p*-xylene and α,α′-dibromo-*m*-xylene, respectively, by the same procedures reported for the preparation of 1,3-bis(1-imidazolyl)-5-(imidazol-1-ylmethyl)-benzene.[12] Elemental analyses of C, H, and N were performed by Galbraith Laboratories, Inc. Thermogravimetric measurements were performed on a TGA Q500 thermal analyzer in the following $N_2$ with the heating rate of 10 °C $min^{-1}$. Calculations were performed using the PM3 semiempirical Hamiltonian,[13] as in the GAMESS suite of programs.[14]

**General Synthesis Conditions.** All hydrothermal syntheses were done in heavy-wall glass tubes constructed in the Chemistry Glass Shop. The tubes, 15 mm × 15 cm (after sealing) with a wall thickness of 2 mm, were filled with materials to approximately 40% of available volume and sealed under vacuum. The sealed tubes were placed in an oven in an isolated room that was preheated to the desired reaction temperature. Table 1 gives the initial molar concentrations of imidazole nitrogen (R-Im), zinc acetate, phosphorous acid, and NaOH. After addition, the relevant species,

(4) (a) Xing, Y.; Liu, Y.; Shi, Z.; Zhang, P.; Fu, Y.; Cheng, C.; Pang, W. *J. Solid State Chem.* **2002**, *163*, 364. (b) Chiang, Y. P.; Kao, H. M.; Lii, K. H. *J. Solid State Chem.* **2001**, *162*, 168. (c) Liu, W.; Liu, Y.; Shi, Z.; Pang, W. *J. Mater. Chem.* **2000**, *10*, 1451. (d) Neeraj, S.; Natarajan, S. *Cryst. Growth Des.* **2001**, *1*. 491. (e) Neeraj, S.; natarajan, S.; Rao, C. N. R. *Chem. Mater.* **1999**, *11*, 1390. (f) Yao, Y. W.; Cui, A. L. *Chem. Lett.* **2001**, 1148. (g) Wiebcke, M. *J. Mater. Chem.* **2002**, *12*, 143. (g) Harrison, W. T. A.; Phillips, M. L. F.; Clegg, W.; Teat, S. J. *J. Solid State Chem.* **1999**, *148*, 433.

(5) (a) Gier, T. E.; Stucky, G. D. *Nature* **1991**, *349*, 508. (b) Feng, P.; Bu, X.; Stucky, G. D. *Angew. Chem., Int. Ed. Engl.* **1995**, *34*, 1745. (c) Neeraj, S.; Natarajan, S. *Chem. Mater.* **2000**, *12*, 2753. (d) Fu, W.; Shi, Z.; Li, G.; Zhang, D.; Dong, W.; Chen, X.; Feng, H. *Solid State Sci.* **2004**, *6*, 225. (e) Yang, G.-Y.; Sevov. S. C. *J. Am. Chem. Soc.* **1999**, *121*, 8389. (f) Zhang, D.; Shi, Z.; Dong, W.; Fu, W.; Wang, L.; Li, G.; Feng, S. *J. Solid State Chem.* **2004**, *177*, 343. (g) Harrison, W. T. A.; Hanooman, L. *Angew. Chem., Int. Ed. Engl.* **1997**, *36*, 640. (h) Yu, J. H.; Yu, W.; Shi, Z. Xu, R. R. *Chem. Mater.* **2001**, *13*, 2972. (i) Jensen, T. R.; Nicolas Gerentes, N.; Jepsen, J.; Hazell, R. G.; Jakobsen, H. J. *Inorg. Chem.* **2005**, in press. (j) Norquist, A. J.; O'Hare, D. *J. Am. Chem. Soc.* **2004**, *126*, 6673. (k) Mandal, S.; Natarajan. S. *Inorg. Chem. Acta* **2004**, *357*, 1437. (l) Song, Y.; Yu, J.; Li, Y.; Zhang, M.; Xu, R. *Eur. J. Inorg. Chem.* **2004**, 3718. (m) Zhang, X. M.; Bai, C. J.; Zhang, Y. L.; Wu, H. S. *Can. J. Chem.* **2004**, *82*, 616. (n) Chen, X.; Wang, Y.; Yu, J.; Zou, Y.; Xu, R. *J. Solid State Chem.* **2004**, *177*, 2518.

(6) (a) Ayi, A. A.; Choudhury, A.; Natarajan, S.; Rao, C. N. R. *J. Mater. Chem.* **2001**, *11*, 1181. (b) Choudhury, A.; Natarajan, S.; Rao, C. N. R. *Inorg. Chem.* **2000**, *39*, 4295. (c) Harrison, W. T. A.; Phillips, M. L. F.; Stanchfield, J.; Nenoff, T. M. *Inorg. Chem.* **2001**, *40*, 895. (d) Drumel, S.; Janvier, P.; Deniaud, D.; Bujoli, B. *J. Chem. Soc., Chem. Commun.* **1995**, 1051. (e) Neeraj, S.; Natarajan, S.; Rao, C. N. R. *New J. Chem.* **1999**, 303. (f) Choudhury, A.; Neeraj, S.; Natarajan, S.; Rao, C. N. R. *J. Mater. Chem.* **2001**, *11*, 1537.

(7) (a) Mellot-Draznieks, C.; Girard, S.; Férey, G.; Schön, J. C.; Cancarevic, Z.; Jansen, M. *Chem.—Eur. J.* **2002**, *8*, 4103. (b) Férey, G. *C. R. Acad. Sci. Paris* **1998**, *Ser. II*, 1.

(8) (a) Kongshaug, K. O.; Fjellvag, H.; Lillerud, K. P. *Solid State Sci.* **2000**, *2*, 569. (b) Natarajan, S. *Solid State Sci.* **2002**, *4*, 1331.

(9) (a) Liu, Y. L.; Na, L. Y.; Zhu, G. S.; Xiao, F. S.; Pang, W. Q.; Xu, R. R., *J. Solid State Chem.* **2000**, *149*, 107. (b) Harrison, W. T. A.; Gier, T. E.; Stucky, G. D.; Broach, R. W.; Bedard, R. A. *Chem. Mater.* **1996**, *8*, 145.

(10) (a) Halasyamani, P. S.; Drewitt M. J.; O'Hare D. *Chem. Commun.* **1997**, 867. (b) Lin, Z.-E.; Zhang, J.; Zheng, S.-T.; Yang, G.-Y. *Microporous Mesporous Mater.* **2004**, *68*, 65. (c) Rodgers J. A.; Harrison, W. T. A. *Chem. Commun.* **2000**, 2385. (d) Liang, J.; Wang, Y.; Yu, J.; Li, Y.; Xu, R. *Chem. Commun.* **2003**, 882. (e) Kirkpatrick, A.; Harrison, W. T. A. *Solid State Sci.* **2004**, *6*, 593.

(11) (a) Dahl, P. K.; Arnold, F. H. *Macromolecules* **1992**, *25*, 7051. (b) Dhal, P. K.; Arnold, F. H. *J. Am. Chem. Soc.* **1991**, *113*, 7417.

(12) Fan, J.; Sun, W. Y.; Okamura, T.-a.; Tang, W. X.; Ueyama, N. *Inorg. Chem.* **2003**, *42*, 3168.

(13) Stewart, J. J. P. *J. Comput. Chem.* **1989**, *10*, 209.

(14) Schmidt, M. W.; Baldridge, K. K.; Boatz, J. A.; Elbert, S. T.; Gordon, M. S.; Jensen, J. H.; Koseki, S.; Matsunaga, N.; Nguyen, K. A.; Su, S. J.; Windus, T. L.; Dupuis, M.; Montogmery, J. A. *J. Comput. Chem.* **1993**, *20*, 1347.

**Table 1.** Initial Molar Concentrations for Syntheses

| compd | R-Im (M) | $Zn(OAc)_2$ (M) | $HPO_3H_2$ (M) | NaOH (M) | temp (°C)/time (d) | yield (%) |
|---|---|---|---|---|---|---|
| **1** | 0.5 | 0.17 | 0.33 | 0 | 130/10 | 84 |
| **2** | 0.17 | 0.083 | 0.17 | 0 | 125/9 | 15 |
| **3** | 0.1 | 0.1 | 0.1 | 0.083 | 125/10 | 14 |
| **4** | 0.1 | 0.1 | 0.1 | 0.083 | 125/10 | 25 |
| **5** | 0.15 | 0.1 | 0.1 | 0.083 | 125/10 | 77 |

**Table 2.** Crystal Data and Structure Refinement Parameters for **1**−**5**[a]

| struct param | **1** | **2** | **3** | **4** | **5** |
|---|---|---|---|---|---|
| empirical formula | $C_4H_7N_2O_3PZn$ | $C_{40}H_{44}N_8O_{12}P_4Zn_4$ | $C_7H_8N_2O_3PZn$ | $C_{14}H_{16}N_4O_6P_2Zn_2$ | $C_{14}H_{16}N_4O_6P_2Zn_2$ |
| fw | 227.46 | 1214.19 | 264.49 | 528.99 | 528.99 |
| *T*/K | 100 | 100 | 100 | 100 | 100 |
| space group | $P2_12_12_1$ | $P\bar{1}$ | $P2_1/c$ | $P2_1/n$ | $P2_1/n$ |
| *a*/Å | 5.2488(5) | 9.6190(6) | 11.2732(13) | 10.8713(9) | 7.6613(5) |
| *b*/Å | 9.6411(8) | 9.6847(6) | 8.8605(9) | 10.1001(7) | 16.3179(11) |
| *c*/Å | 14.5214(13) | 26.2565(16) | 9.9607(11) | 18.2501(11) | 14.5275(10) |
| $\alpha$/deg | 90 | 100.260(5) | 90.00 | 90 | 90 |
| $\beta$/deg | 90 | 100.104(5) | 110.166(10) | 90.285(6) | 92.866(6) |
| $\gamma$/deg | 90 | 90.091(3) | 90.00 | 90 | 90 |
| *V*/Å$^3$ | 734.84(11) | 2368.2(3) | 933.94(18) | 2003.9(2) | 1813.9(2) |
| Z | 4 | 2 | 4 | 4 | 4 |
| $D_{calc}$/g cm$^{-3}$ | 2.056 | 1.703 | 1.881 | 1.753 | 1.937 |
| $\mu$/mm$^{-1}$ | 3.515 | 2.205 | 2.781 | 2.592 | 2.863 |
| $R_1$[a] [$I > 2\sigma(I)$] | 0.0282 | 0.0603 | 0.0641 | 0.0424 | 0.0255 |
| $wR_2$[b] [$I > 2\sigma(I)$] | 0.0667 | 0.1610 | 0.1675 | 0.0909 | 0.0633 |

[a] $R_1 = \Sigma|F_o| - |F_c|/\Sigma|F_o|$. [b] $wR_2 = \{\Sigma[w(F_o^2 - F_c^2)^2]/\Sigma[w(F_o^2)^2]\}^{1/2}$, where $w = 1/[\sigma^2(F_o)^2 + (aP)^2 + bP]$ and $P = [(F_o)^2 + 2(F_c)^2]/3$.

R-Im$H^+$ and $HPO_3H^-$, and acetic acid have p$K_a$s in the range 4.7−6.9. The initial pH, as determined by paper indicator, for each reaction was in the range 6−8 as expected from the compositions. After the reaction the pH values were found to be in the 6−8 range. The reactions appear to be effectively buffered by the presence of the ligand and all other reaction components.

**$[Zn(HPO_3)(C_4H_6N_2)]$ (1).** Hydrothermal treatment of zinc acetate dihydrate (219.5 mg, 1.0 mmol), phosphorous acid (164.0 mg, 2.0 mmol), 1-methylimidazole (246.1 mg, 3.0 mmol), and distilled water (6 mL) for 10 days at 130 °C yields a colorless crystalline product. Yield: 84% on the basis of zinc source. FT-IR (cm$^{-1}$): 3122 (w), 2368 (m), 1542 (m), 1527 (m), 1289 (w), 1239 (w), 1145 (s), 1110 (s), 1084 (s), 1044 (s), 1030 (s), 1007 (s), 953 (s), 866 (w), 835 (s), 778 (s), 675 (w). Anal. Calcd for $C_4H_7N_2O_3PZn$: C, 21.12; H, 3.10; N, 12.32. Found: C, 21.03; H, 3.42; N, 11.76.

**$[Zn_2(HPO_3)_2(C_{10}H_{10}N_2)_2]_2$ (2).** Hydrothermal treatment of zinc acetate dihydrate (109.8 mg, 0.5 mmol), phosphorous acid (82.0 mg, 1.0 mmol), 1-benzylimidazole (158.2 mg, 1.0 mmol), and distilled water (6 mL) for 9 days at 125 °C yields a colorless crystalline product. Yield: 15% on the basis of zinc source. FT-IR (cm$^{-1}$): 3105 (w), 2356 (m), 1528 (m), 1444 (w), 1358 (w), 1284 (m), 1244 (m), 1155 (m), 1100 (s), 1028 (s), 1008 (s), 950 (m), 873 (m), 860 (m), 825 (m), 782 (w), 738 (m), 711 (s), 692 (m). Anal. Calcd for $C_{40}H_{44}N_8O_{12}P_4Zn_4$: C, 39.57; H, 3.65; N, 9.23. Found: C, 39.73; H, 3.98; N, 9.20.

**$[Zn(HPO_3)(C_{14}H_{14}N_4)_{0.5}]$ (3).** Hydrothermal treatment of zinc acetate dihydrate (131.8 mg, 0.6 mmol), phosphorous acid (49.2 mg, 0.6 mmol), sodium hydroxide (20.0 mg, 0.5 mmol), 1,4-bis-(imidazol-1-ylmethyl)benzene (71.4 mg, 0.3 mmol), and distilled water (6 mL) for 10 days at 125 °C yields a block crystalline product, accompanied by an unknown powder product. Yield: 14% on the basis of zinc source. FT-IR (cm$^{-1}$): 3107 (m), 2381 (m), 1530 (m), 1454 (w), 1355 (w), 1285 (w), 1245 (m), 1168 (w), 1147 (s), 1115 (s), 1095 (s), 1082 (s), 1029 (s), 1006 (s), 950 (m), 879 (m), 864 (m), 739 (m), 718 (m). Anal. Calcd for $C_7H_8N_2O_3PZn$: C, 31.79; H, 3.05; N, 10.59. Found: C, 30.91; H, 3.13; N, 10.20.

**$[Zn_2(HPO_3)_2(C_{14}H_{14}N_4)]\cdot 0.4H_2O$ (4).** Hydrothermal treatment of zinc acetate dihydrate (65.9 mg, 0.3 mmol), phosphorous acid (49.2 mg, 0.6 mmol), sodium hydroxide (20.0 mg, 0.5 mmol), 1,3-bis(imidazol-1-ylmethyl)benzene (71.4 mg, 0.3 mmol), and distilled water (6 mL) for 10 days at 125 °C yields a plate crystalline product and a block crystalline material, compound **5**, as evidenced by X-ray powder diffraction. Yield: about 25% on the basis of zinc source. FT-IR (cm$^{-1}$): 3125 (m), 2353 (m), 1523 (m), 1448 (w), 1400 (w), 1274 (w), 1235 (m), 1148 (s), 1086 (s), 1028 (s), 1004 (s), 949 (s), 894 (w), 834 (m), 820 (m), 772 (m), 752 (m), 742 (m), 722 (s), 677 (w). Anal. Calcd for $C_{14}H_{16.8}N_4O_{6.4}P_2Zn_2$: C, 31.36; H, 3.16; N, 10.45. Found: C, 31.13; H, 3.30; N, 10.16. To confirm the noncoordinated water content, thermogravimetric measurements using a TGA Q500 thermal analyzer were performed on a crystalline product of **3** in the following $N_2$ with the heating rate of 10 °C min$^{-1}$. The weight loss (32 to ∼160 °C) corresponds to the loss of noncoordinated water molecules (obsd 1.6%, 0.44 $H_2O$; calcd 1.5%). This compound is stable up to 300 °C as shown in the TGA curve.

**$[Zn_2(HPO_3)_2(C_{14}H_{14}N_4)]$ (5).** Hydrothermal treatment of zinc acetate dihydrate (65.9 mg, 0.3 mmol), phosphorous acid (49.2 mg, 0.6 mmol), sodium hydroxide (20.0 mg, 0.5 mmol), 1,3-bis-(imidazol-1-ylmethyl)benzene (107.1 mg, 0.45 mmol), and distilled water (6 mL) for 10 days at 125 °C yields a block crystalline product. Yield: 77% on the basis of zinc source. FT-IR (cm$^{-1}$): 3122 (w), 2358 (m), 1534 (m), 1516 (m), 1438 (w), 1277 (w), 1231 (w), 1189 (s), 1135 (s), 1109 (s), 1082 (s), 1022 (s), 1007 (s), 952 (m), 847 (m), 826 (m), 817 (m), 767 (m), 747 (m), 715 (m), 670 (w). Anal. Calcd for $C_{14}H_{16}N_4O_6P_2Zn_2$: C, 31.79; H, 3.05; N, 10.59. Found: C, 31.89; H, 3.33; N, 10.35.

**Crystallographic Analyses.** Low-temperature (100 K) single-crystal X-ray diffraction measurements for compounds **1**−**5** were collected on a Oxford Diffraction Xcalibur2 diffractometer equipped with the Enhance X-ray source and a Sapphire 2 CCD detector. The data collection routine, unit cell refinement, and data processing were carried out with the program CrysAlis.[15] The structures were solved by SHELXS-97 and refined by full-matrix least squares. The final refinements involved an anisotropic model for all non-

(15) *CrysAlis v1.171*; Oxford Diffraction: Wroclaw, Poland, 2004.

**Table 3.** Selected Bond Distances (Å) and Angles (deg) for **1**−**5**[a]

| | | | |
|---|---|---|---|
| Compound **1** | | | |
| Zn1−N1 | 2.0153(19) | Zn1−O1 | 1.9389(17) |
| Zn1−O2$^{\#1}$ | 1.9357(16) | Zn1−O3$^{\#2}$ | 1.9371(16) |
| O2$^{\#1}$−Zn1−O3$^{\#2}$ | 109.71(7) | O2$^{\#1}$−Zn1−O1 | 113.72(7) |
| O3$^{\#2}$−Zn1−O1 | 113.96(7) | O2$^{\#1}$−Zn1−N1 | 107.08(8) |
| O3$^{\#2}$−Zn1−N1 | 109.97(7) | O1−Zn1−N1 | 101.88(7) |
| P1−O1−Zn1 | 134.20(10) | P1−O2−Zn1$^{\#2}$ | 129.64(10) |
| P1−O3−Zn1$^{\#1}$ | 128.14(10) | | |
| Compound **2** | | | |
| Zn1−O3 | 1.929(3) | Zn1−O4 | 1.936(3) |
| Zn1−O6$^{\#3}$ | 1.949(3) | Zn1−N1 | 2.002(4) |
| Zn2−O5 | 1.914(3) | Zn2−O2$^{\#4}$ | 1.934(3) |
| Zn2−O1$^{\#5}$ | 1.944(3) | Zn2−N3 | 1.990(4) |
| Zn3−O8$^{\#6}$ | 1.916(3) | Zn3−O12$^{\#7}$ | 1.932(3) |
| Zn3−O11 | 1.946(3) | Zn3−N5 | 1.984(4) |
| Zn4−O7$^{\#8}$ | 1.948(3) | Zn4−O10 | 1.928(3) |
| Zn4−O9 | 1.947(3) | Zn4−N7 | 1.989(4) |
| O3−Zn1−O4 | 101.96(14) | O3−Zn1−O6$^{\#3}$ | 110.89(15) |
| O4−Zn1−O6$^{\#3}$ | 106.05(13) | O3−Zn1−N1 | 112.47(15) |
| O4−Zn1−N1 | 116.00(14) | O6$^{\#3}$−Zn1−N1 | 109.14(15) |
| O5−Zn2−O2$^{\#4}$ | 105.62(16) | O5−Zn2−O1$^{\#5}$ | 103.31(15) |
| O2$^{\#4}$−Zn2−O1$^{\#5}$ | 107.50(16) | O5−Zn2−N3 | 115.47(15) |
| O2$^{\#4}$−Zn2−N3 | 110.40(15) | O1$^{\#5}$−Zn2−N3 | 113.86(15) |
| O8$^{\#6}$−Zn3−O12$^{\#7}$ | 105.33(15) | O8$^{\#6}$−Zn3−O11 | 105.51(15) |
| O12$^{\#7}$−Zn3−O11 | 106.08(14) | O8$^{\#6}$−Zn3−N5 | 115.56(15) |
| O12$^{\#7}$−Zn3−N5 | 113.57(14) | O11−Zn3−N5 | 110.05(15) |
| O10−Zn4−O9 | 101.02(14) | O10−Zn4−N7 | 112.44(15) |
| O9−Zn4−N7 | 115.59(14) | O10−Zn4−O7$^{\#8}$ | 110.07(14) |
| O9−Zn4−O7$^{\#8}$ | 107.61(13) | O7$^{\#8}$−Zn4−N7 | 109.70(15) |
| P2−O4−Zn1 | 131.42(19) | P1−O3−Zn1 | 143.1(2) |
| P2−O5−Zn2 | 144.1(2) | P3−O9−Zn4 | 130.81(19) |
| P4−O11−Zn3 | 134.5(2) | P4−O10−Zn4 | 143.6(2) |
| Compound **3** | | | |
| Zn1−O2 | 1.918(3) | Zn1−O3 | 1.928(3) |
| Zn1−O1 | 1.943(3) | Zn1−N1 | 1.999(4) |
| O2−Zn1−O3 | 101.96(13) | O2−Zn1−O1 | 112.10(13) |
| O3−Zn1−O1 | 109.36(13) | O2−Zn1−N1 | 111.49(14) |
| O3−Zn1−N1 | 114.66(15) | O1−Zn1−N1 | 107.31(14) |
| P1−O3−Zn1 | 127.63(18) | P1$^{\#9}$−O2−Zn1 | 140.3(2) |
| P1$^{\#10}$−O1−Zn1 | 129.51(17) | | |
| Compound **4** | | | |
| Zn1−O6 | 1.920(3) | Zn1−O1$^{\#11}$ | 1.940(2) |
| Zn1−O3 | 1.948(3) | Zn1−N31$^{\#12}$ | 1.998(3) |
| Zn2−O4 | 1.937(3) | Zn2−O5$^{\#13}$ | 1.937(3) |
| Zn2−O2 | 1.943(3) | Zn2−N11 | 1.987(3) |
| O6−Zn1−O1$^{\#11}$ | 106.78(12) | O6−Zn1−O3 | 115.07(12) |
| O1$^{\#11}$−Zn1−O3 | 98.21(10) | O6−Zn1−N31$^{\#12}$ | 113.77(13) |
| O1−Zn1−N31$^{\#12}$ | 108.20(12) | O3−Zn1−N31$^{\#12}$ | 113.18(13) |
| O4−Zn2−O5$^{\#13}$ | 112.93(11) | O4−Zn2−O2 | 110.32(11) |
| O5$^{\#13}$−Zn2−O2 | 104.58(11) | O4−Zn2−N11 | 110.94(12) |
| O5$^{\#13}$−Zn2−N11 | 107.39(12) | O2−Zn2−N11 | 110.47(12) |
| P2−O4−Zn2 | 135.69(16) | P2−O6−Zn1 | 138.03(17) |
| P1−O2−Zn2 | 121.74(15) | P1−O3−Zn1 | 121.30(15) |
| Compound **5** | | | |
| Zn1−O1 | 1.9163(13) | Zn1−O6 | 1.9449(13) |
| Zn1−N11 | 2.0009(15) | Zn1−N31$^{\#14}$ | 2.0074(15) |
| Zn2−O2 | 1.9335(13) | Zn2−O3$^{\#15}$ | 1.9410(13) |
| Zn2−O5$^{\#16}$ | 1.9527(13) | Zn2−O4 | 1.9290(13) |
| O1−Zn1−O6 | 111.26(6) | O1−Zn1−N11 | 105.95(6) |
| O6−Zn1−N11 | 112.46(6) | O1−Zn1−N31$^{\#14}$ | 113.92(6) |
| O6−Zn1−N31$^{\#14}$ | 100.48(6) | N11−Zn1−N31$^{\#14}$ | 112.94(6) |
| O4−Zn2−O2 | 116.62(6) | O4−Zn2−O3$^{\#15}$ | 108.11(6) |
| O2−Zn2−O3$^{\#15}$ | 116.65(6) | O4−Zn2−O5$^{\#16}$ | 109.98(6) |
| O2−Zn2−O5$^{\#16}$ | 104.25(6) | O3−Zn2−O5$^{\#16}$ | 99.66(6) |
| P2−O4−Zn2 | 135.79(8) | P2−O6−Zn1 | 119.94(7) |
| P1−O2−Zn2 | 141.69(9) | P1−O1−Zn1 | 141.07(9) |

[a] Symmetry transformations used to generate equivalent atoms: #1, $x + 1/2, -y + 7/2, -z$; #2, $x - 1/2, -y + 7/2, -z$; #3, $-x + 2, -y, -z$; #4, $-x + 2, -y + 1, -z$; #5, $x + 1, y, z$; #6, $-x + 1, -y + 2, -z + 1$; #7, $-x + 1, -y + 1, -z + 1$; #8, $-x, -y + 2, -z + 1$; #9, $x, -y + 3/2, z + 1/2$; #10, $-x + 1, -y + 1, -z$; #11, $-x - 1, y + 1/2, -z + 3/2$; #12, $-x, -y + 1, -z + 1$; #13, $-x - 1, -y + 1, -z + 1$; #14, $-x + 3/2, y + 1/2, -z + 3/2$; #15, $-x + 2, -y + 1, -z + 1$; #16, $-x + 1, -y + 1, -z + 1$.

hydrogen atoms.[16] The refinement of the Flack absolute parameter in **1** to −0.001(10) indicated that the absolute structure is well defined. A noncoordinated water oxygen with a site occupancy factor of 0.44 was found in the structural channel of **4**. The hydrogen atom bonded to this oxygen atom was not located. In **1**−**5**, the hydrogen atoms attached to the phosphorus group were located from the residual $e^-$ density map and refined independently, and the hydrogen atoms attached to the organic ligand were added by the expected geometry. The crystal parameters, data collection parameters, and refinement results for compounds **1**−**5** are summarized in Table 2. Selected bond length and angles are listed in Table 3. Further details are provided in the Supporting Information.

## Results and Discussion

**Description of the Crystal Structures. [Zn(HPO$_3$)(C$_4$H$_6$N$_2$)] (1) and [Zn$_2$(HPO$_3$)$_2$(C$_{10}$H$_{10}$N$_2$)$_2$]$_2$ (2).** The asymmetric unit of compound **1** contains one zinc atom, one phosphite, and one 1-methylimidazole as shown in Figure 1a. Each zinc atom in compound **1** is coordinated by three oxygen atoms from three different phosphite groups and one nitrogen atom from 1-methylimidazole to complete its tetrahedral coordination environment. Compound **1** is closely related to $C_4N_2O_3H_8 \cdot ZnHPO_3$[3a] ($C_4N_2O_3H_8$ = L-asparagine), which crystallizes in the same space group $P2_12_12_1$ and has a similar 1D ladder structure but with the tetrahedral coordination geometry of the zinc atom defined by four oxygen atoms. The zinc coordination mode in compound **1** has typical geometrical parameters: $(Zn-O)_{av} = 1.94$ Å, and O−Zn−O bond angles are in the range of 109.7−114.0° with an average value of 112.5°. The O−Zn−N bond angles are in the range 101.9−110.0° with an average value of 106.3°. The phosphorus atom bonds to three oxygen atoms [$d_{av}$(P−O) = 1.52 Å] with the fourth tetrahedral vertex occupied by a hydrogen atom. The three bridging O atoms have an average Zn−O−P bond angle of 130.7°.

The $ZnO_3N$ and $HPO_3$ groups are connected to form an edge-shared ladder structure of 4-rings that propagates along the [100] direction (Figure 1b). The 1-methylimidazole ligands are attached to the zinc atoms and extend to each side of the ladder structure. The neutral chains in compound **1** are held together by van der Waals forces. A packing diagram is included in the Supporting Information.

The asymmetric unit of compound **2** contains two crystallographically independent motifs. Each motif contains two zinc atoms, two phosphite units, and two 1-benzylimidazole groups (Figure 2a). Each zinc atom is tetrahedrally coordinated by three oxygen atoms from three different phosphite groups and one nitrogen atom from one 1-benzylimidazole. In **2**, the O−Zn−O bond angles are in the range of 101.0−110.9°, and O−Zn−N bond angles are in the range 109.1−116.0°. Each phosphite group in compound **2** bridges three zinc atoms with the Zn−O distance ranging from 1.914(3) to 1.949(3) Å.

Unlike the chain structure in compound **1**, the $ZnO_3N$ and $HPO_3$ groups in **2** are connected to form a 2D sheet, as

(16) (a) Sheldrick, G. M. *SHELXS97, Program for Crystal Structure Determination*; University of Göttingen: Göttingen, Germany, 1997. (b) Sheldrick, G. M. *SHELXL97, Program for Crystal Structural Refinement*; University of Göttingen: Göttingen, Germany, 1997.

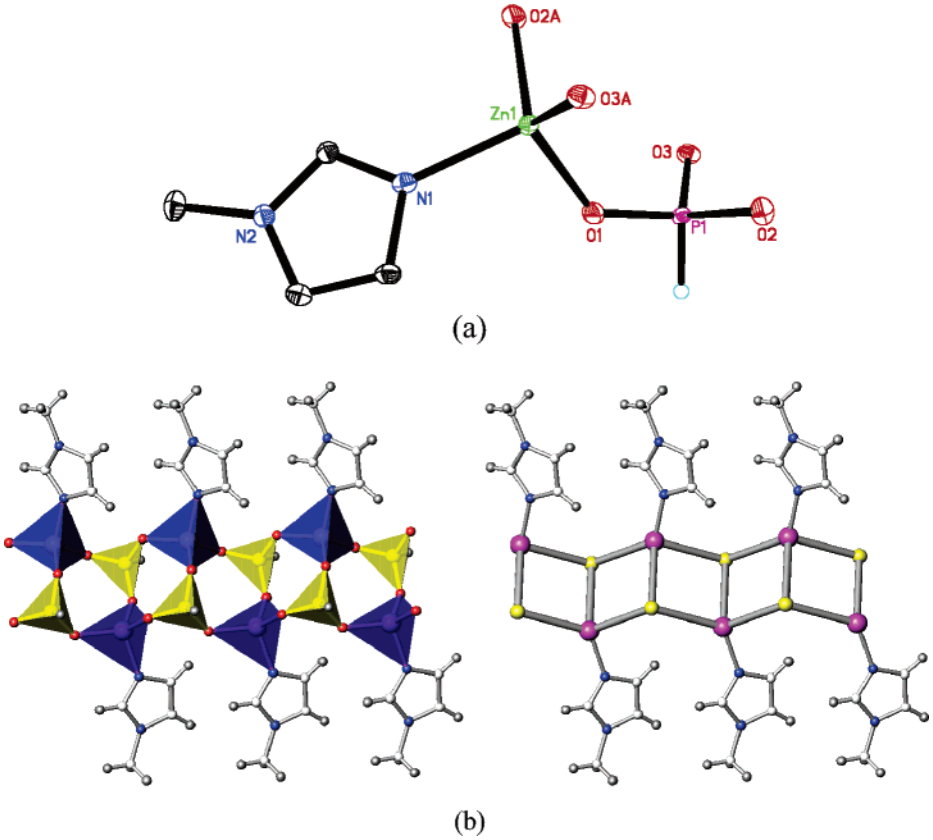


**Figure 1.** (a) ORTEP plot of the asymmetric unit of compound **1** showing the atom-labeling scheme. The ellipsoids are drawn at the 50% probability level. Two additional symmetry-related atoms are indicated by O2A and O3A. (b) Ladder structure of compound **1**: (left) connectivity of the $HPO_3$ (yellow) and $ZnO_3N$ (blue) tetrahedra; (right) zigzag arrangement of 4-rings with Zn−O−P linkage drawn by a single line.

illustrated in Figure 2b. Zinc tetrahedra and phosphorus tetrahedra are connected to form 4-rings and 8-rings. Each 4-ring is surrounded by four 8-rings, and each 8-ring is surrounded by four 4-rings. Thus, the 2D network has a $4.8^2$ topology.[2f,12] Recently, a 2-fold interpenetrated zinc phosphite framework connected by ethylenediamine was reported, in which the inorganic sheets are of the same $4.8^2$ topology and the ethylenediamine groups pass through the 8-rings to connect alternating sheets.[10c] In the case of **2**, the 1-benzylimidazole ligands that coordinate zinc and extend to each side of the sheet with the benzene ring nearly perpendicular to the inorganic sheet. The opening of the 8-ring is about 6.7 × 5.8 Å, which is too small to allow the benzene rings to pass through. Within each 2D sheet of compound **2**, the 4-rings are not parallel to each other (Figure 2b) and a helical chain can be extracted from this layer structure as reported previously for $4.8^2$ rings.[10d] The layer that contains Zn(1) and Zn(2) atoms forms an independent sheet, A, and the layer that contains Zn(3) and Zn(4) atoms forms an adjacent sheet, B. The two kinds of sheets are packed in an ABAB mode, and the topology of each sheet is identical.

Both **1** and **2** are built from monodentate imidazole ligands, 1-methylimidazole and 1-benzylimidazole, respectively. Thus, it is interesting to note the role of the benzene ring in defining the structure of **2**. The ladder structure is commonly observed with monodendate and bridging ligands and appears to be a stable structure under hydrothermal synthesis conditions.[6a,17] Compound **1**, for example, is formed in 84% yield. The addition of a benzene ring to methylimidazolyl to form benzylimidazole apparently is not readily accommodated by a ladder structure. It is likely that the C−H···$\pi$ interactions[18] drive the formation of a layer structure in **2** and that the layered structure observed maximizes benzene−benzene interactions. The C−H−X (X refers to the centroid of the benzene ring) angles range from 145.2 to 171.7°, and the H···X distances range from 2.64 to 3.21 Å. A figure illustrating the C−H···$\pi$ interaction between benzene rings is included in the Supporting Information.

Further, if each pair of benzene rings involved in C−H···$\pi$ interactions is taken as a single unit, then the 3D structure of compound **2** can be regarded as a pillared layer structure. Namely, the inorganic sheets are supported by a pseudo-bis(imidazole) ligands. To further elaborate the role of bis(imidazole) ligands in the formation of the hybrid inorganic/organic zinc phosphite materials, we investigated the reactions of 1,4-bis(imidazol-1-ylmethyl)benzene and 1,3-bis(imidazol-1-ylmethyl)benzene with zinc phosphites. Three new compounds with unique architectures are formed. In **3** and **4**, inorganic zinc phosphite sheets are pillared by the

(17) Fan, J.; Slebodnick, C.; Angel. R.; Hanson, B. E. *Inorg. Chem.* **2005**, in press.

(18) (a) Choudhury, A. R.; Islam, K.; Kirchner, M. T.; Mehta, G.; Row, T. N. G. *J. Am. Chem. Soc.* **2004**, *126*, 12274. (b) Caradoc-Davies, P. L.; Gregory, D. H.; Hanton, L. R.; Turnbull, J. M. *J. Chem. Soc., Dalton Trans.* **2002**, 1574. (c) Jitsukawa, K.; Iwai, K.; Masuda, H.; Ogoshi, H.; Einaga, H. *J. Chem. Soc., Dalton Trans.* **1997**, 3691. (d) Zhu, H. F.; Kong, L. Y.; Okamura, T.-a.; Fan, J.; Sun, W. Y.; Ueyama, N. *Eur. J. Inorg. Chem.* **2004**, 1465.

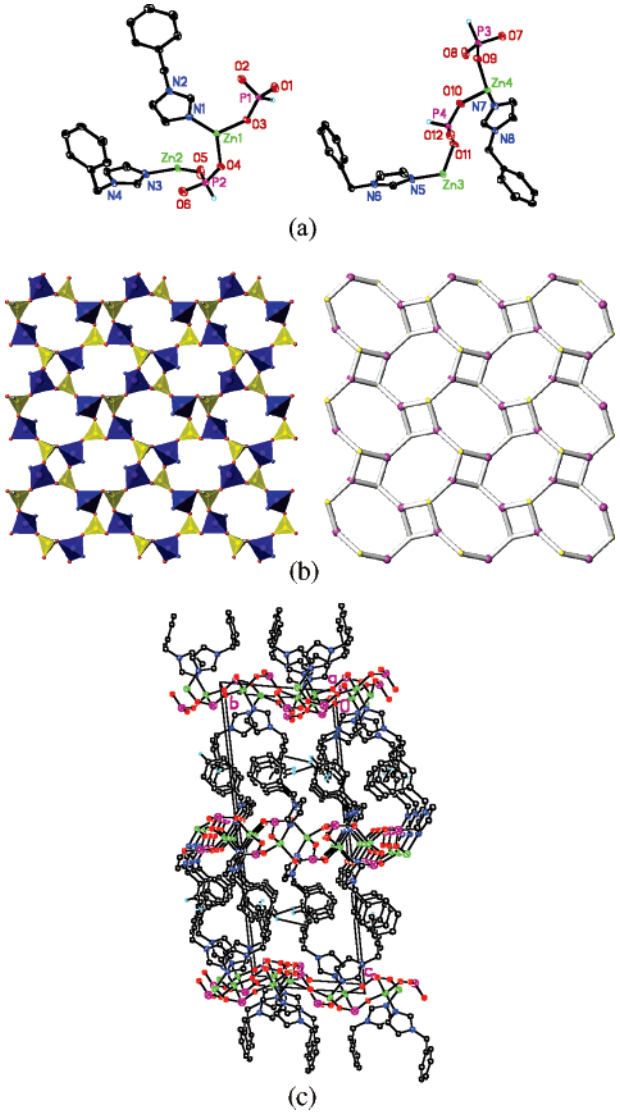


**Figure 2.** (a) ORTEP plot of the asymmetric unit of compound **2** showing the atom-labeling scheme. The ellipsoids are drawn at the 50% probability level. Symmetry-related atoms are indicated by O1A, etc. (b) 2D structure of compound **2**: (left) connectivity of $HPO_3$ (yellow) and $ZnO_3N$ (blue) tetrahedra to 4-ring and 8-ring loops; (right) schematic drawing of the 2D $4.8^2$ network. (c) Crystal packing diagram for compound **2** with the C−H···$\pi$ interactions indicated by dashed lines.

bis(imidazole) ligand to form a 3D structure, and in **5**, inorganic zinc phosphite chains are linked by the ligand to generate a 3D structure.

**Compounds $[Zn(HPO_3)(C_{14}H_{14}N_4)_{0.5}]$ (3), $[Zn_2(HPO_3)_2(C_{14}H_{14}N_4)]\cdot 0.4H_2O$ (4), and $[Zn_2(HPO_3)_2(C_{14}H_{14}N_4)]$ (5).** The asymmetric unit of **3** contains one zinc atom, one phosphite unit, and a half 1,4-bis(imidazol-1-ylmethyl)-benzene ligand (Figure 3a). The zinc atoms in **3** are tetrahedrally coordinated by three oxygen atoms and one nitrogen atom as in **2**. It is interesting to note that the $ZnO_3N$ and $HPO_3$ groups are connected to form the same topology, namely $4.8^2$, as in **2**. Furthermore, the layer structure is connected by the organic ligand to form a pillared structure as shown in Figure 3b. In **3**, the two imidazole groups of the ligand extend to both sides of the benzene ring, with a dihedral angle between the benzene ring and the imidazole plane of 74.3°. Thus, the bis(imidazole) ligand in **3** adopts

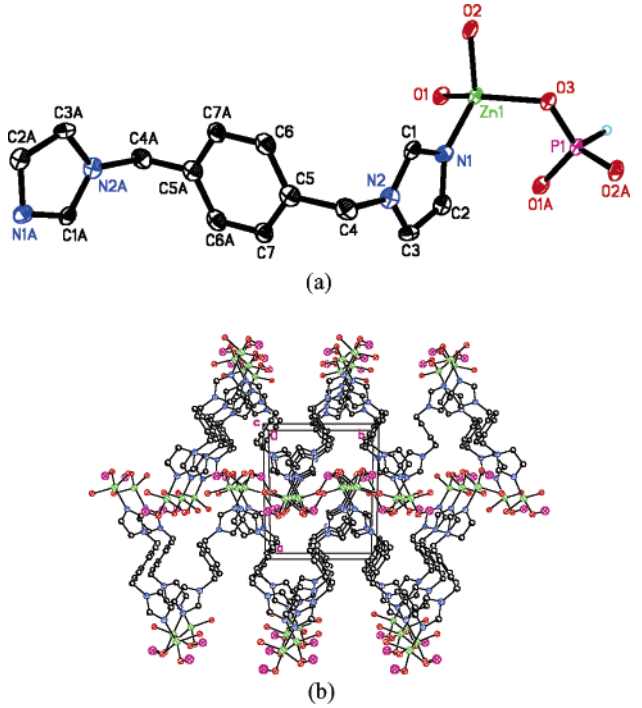


**Figure 3.** (a) ORTEP plot of the asymmetric unit of compound **3** showing the atom-labeling scheme. The ellipsoids are drawn at the 50% probability level. Symmetry-related atoms are indicated by O1A, etc. (b) Crystal packing diagram for compound **3**.

a trans-conformation. In **3**, the organic ligands are held together via weak C−H···$\pi$ interactions. A packing diagram is included with the Supporting Information. The C−H−X (X refers to the centroid of the benzene ring) angle is 128.7°, and the H···X distance is 3.02 Å. Recently, Feng and co-workers reported two 3D zinc phosphites, $[C_6H_4(CH_2NH_3)_2]\cdot[Zn_3(HPO_3)_4]$ and $[CH_3CH_2CH_2NH_3]_2\cdot[Zn_3(HPO_3)_4]$, in which the inorganic layers with similar topology as in **3** are connected by inorganic chains and not by organic groups as in **3**.[5f]

The asymmetric unit of **4** contains two zinc atoms, two phosphite units, one 1,3-bis(imidazol-1-ylmethyl)benzene, and one partially occupied noncoordinated water molecule. As shown in Figure 4a, each zinc atom in **4** has the same coordination environment as observed in **1**−**3**, namely tetrahedrally coordinated by three oxygen atoms and one nitrogen atom.

In **4**, the $ZnO_3N$ and $HPO_3$ groups are connected to form a triple fused 4-rings, and four triple fused 4-rings are held together to generate a 12-ring (Figure 4b). Within one 12-ring, the shortest distance between the diagonal zinc atoms is 7.44 Å. The free space within the 12-ring is greatly reduced because the Zn−N bonds attached to these two zinc atoms extend toward the center of the 12-ring. The alternating triple-fused 4-rings and 12-rings form an unusual 2D inorganic sheet. The most common ring patterns in zinc phosphites are 4-rings and 8-rings,[2f,10,11] and although 12-rings are known in framework structures,[2d,4c,20] the 12-ring pattern of **4** has not previously been observed. In **4**, the two imidazole groups of the ligand extend to the same side of the benzene ring, with a dihedral angle between these two rings of 57.7°. Thus the bis(imidazole) ligand in **4** adopts a cis-conformation

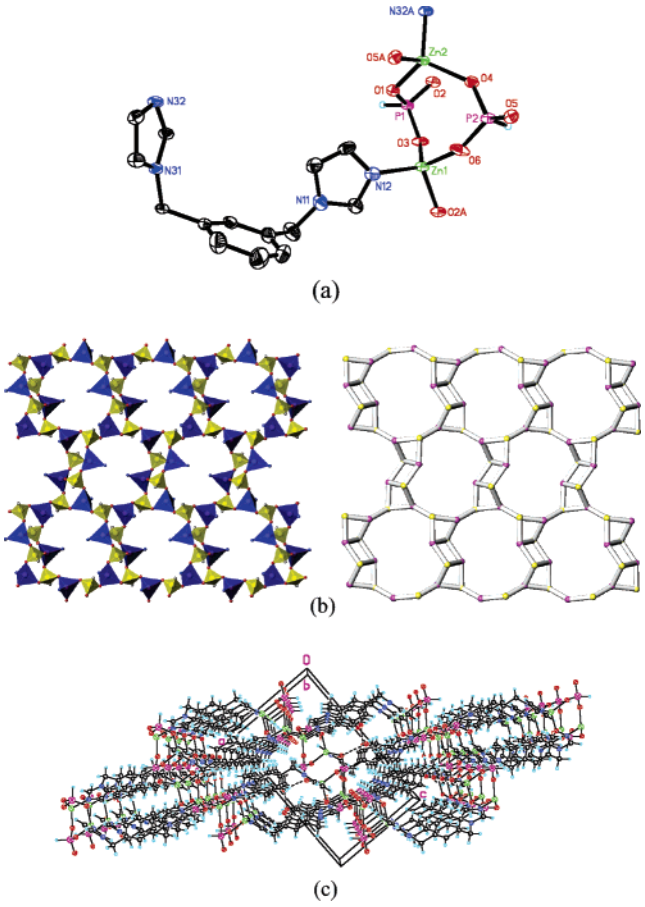


**Figure 4.** (a) ORTEP plot of the asymmetric unit of compound **4** showing the atom-labeling scheme. The ellipsoids are drawn at the 50% probability level. Three additional symmetry-related atoms are indicated by N31A, O5A, and O1A. (b) 2D inorganic framework of compound **4**: (left) connectivity of the $HPO_3$ (yellow) and $ZnO_3N$ (blue) tetrahedra to the triple fused 4-rings and 12-ring loops; (right) schematic drawing of the 2D network. (c) Crystal packing diagram for compound **4** with the hydrogen bond indicted by dashed lines.

and connects adjacent sheets to form the pillared layer structure (Figure 4c). The benzene ring of the ligand is essentially perpendicular to the inorganic layer as in **2**, which results in a large interlayer spacing of 11.47 Å. Noncoordinated water molecules are located within the structural channels, which are hydrogen bonded to a phosphite oxygen atom as indicated by the O1w···O5 ($x + 1, y - 1, z$) distance of 2.81 Å. The distance between the benzene ring and the neighboring imidazole ring is 4.09 Å with the dihedral angle of 14.8°. This implies the occurrence of weak $\pi\cdots\pi$ interactions, and the organic ligands are connected to form a 1D zigzag chain along the *c* axis.[21]

Interestingly, compound **5** is synthesized under reaction conditions similar to those of compound **4**, i.e., the same ligand, reaction temperature, and time, but with a different ligand-to-zinc ratio (see Experimental Section). The structures of **4** and **5**, however, are quite different. Due to its flexibility, the bis(imidazole) ligand can adopt subtly different conformations to meet the geometrical requirement of metal ions, leading to the formation of **4** and **5**. Additionally, the triple 4-ring pattern shows different degree of distortion in the two compounds (see below).

The asymmetric unit of compound **5** contains two zinc atoms, phosphite units, and one 1,3-bis(imidazol-1-ylmethyl)-benzene, which repeat to form the framework (Figure 5a). In **5**, Zn2 atom is coordinated by four oxygen atoms from four different phosphite groups, $ZnO_4$ [$d_{av}$(Zn−O) = 1.94 Å], and Zn1 is coordinated by two oxygen atoms from two different phosphite groups [$d_{av}$(Zn−O) = 1.93 Å] and two nitrogen atoms from two different ligands [$d_{av}$(Zn−N) = 2.00 Å].

In **5**, the $ZnO_3N$ and $HPO_3$ groups are connected to form a triple-fused 4-rings (A−C loops), which are held together to generate a 1D chain via Zn−O−P linkages (Figure 5b). A visual way of describing the 1D chain is that it consists of triple-fused 4-rings, which are held together in a stair-step pattern. A similar stair step structure is formed in a related compound $[(C_6N_4H_{22})_{0.5}]^{2+}[Zn_2(HPO_4)]^{2-}$;[4c] the stair steps in this structure are further linked by Zn−O−P linkages to form 2D sheets that contain 12-rings. In **5**, however each 1D chain is connected to four neighboring chains by the organic ligand to form the 3D structure. The chains propagate along the *a* axis. The ligand in **5** adopts a cis conformation as in **4**, with the dihedral angle between the two imidazole rings of 107.7°. A packing diagram is included in the Supporting Information.

In compounds **4** and **5**, the two terminal 4-rings of the triple fused 4-rings extend to the each side of the central 4-ring. Thus, the triple 4-rings adopt a trans conformation (Figure 6). In **4**, the four T (T = Zn, P) atoms of the central 4-ring are coplanar while the T atoms of the terminal rings are not. The terminal rings adopt a butterfly structure with dihedral angles of 127.1 and 123.3°, respectively, between the trigonal planes, and the dihedral angles between the central ring and its neighboring trigonal planes are 109.1 and 146.2°, respectively (Figure 6a). In **5**, the corresponding dihedral angles are 164.7, 165.7, 107.6, and 96.9°, respectively (Figure 6b). That is, the triple 4-rings in **5** are less distorted than in **4**. The relationship between the triple 4-rings in the chain structure of **5** and the triple 4-rings in the sheet structure of **4** is depicted in Scheme 2. Starting from **4**, (I) the two connected triple 4-rings units may be cleaved into two independent units, (II) one triple 4-ring is rotated and

(19) (a) Phillips, M. L. F.; Nenoff, T. M.; Thompson, C. T.; Harrison, W. T. A. *J. Solid State Chem.* **2002**, *167*, 337. (b) Dong, W.; Li, G.; Shi, Z.; Fu, W.; Zhang, D.; Chen, X.; Dai, Z.; Wang, L.; Feng, S. *Inorg. Chem. Chem.* **2003**, *6*, 776. (c) Gordon, L. E.; Harrison, W. T. A. *Acta Crystallogr.* **2004**, *C60*, m637.

(20) (a) Jensen, T. R.; Hazell, R. F. *J. Chem. Soc., Dalton Trans.* **2000**, 2831. (b) Ayi, A. A.; Choudhury, A.; Natarajan, S.; Rao, C. N. R. *J. Mater. Chem.* **2000**, *10*, 2606. (c) Harrison, W. T. A.; Phillips, M. L. F.; Nenoff, T. M. *J. Chem. Soc., Dalton Trans.* **2001**, 2459. (d) Harrison, W. T. A.; Bircsak, Z.; Hannooman, L.; Zhang, Z. *J. Solid State Chem.* **1998**, *136*, 93. (e) Harrison, W. T. A.; Phillips, M. L. F. *Chem. Mater.* **1997**, *9*, 1837. (f) Wang, Y.; Yu, J.; Guo, M.; Xu, R. *Angew. Chem., Int. Ed.* **2003**, *42*, 4089. (g) Cui, A.; Yao, Y. *Chem. Lett.* **2001**, 1148. (h) Chidambaram, D.; Neeraj, S.; Natarajan, S.; Rao, C. N. R. *J. Solid State Chem.* **1999**, *147*, 154. (i) Kongshaug, K. O.; Fjellvag, H.; Lillerud, K. P. *Microporous Mesporous Mater.* **2000**, *39*, 341. (j) Fu, W.; Shi, Z.; Zhang, D.; Li, G.; Dai, Z.; Chen, X.; Feng, S. *J. Solid State Chem.* **2003**, *174*, 11. (k) Zhang, P.; Wang, Y.; Zhu, G.; Shi, Z.; Liu, Y.; Yuan, H.; Pang, W. *J. Solid State Chem.* **2000**, *154*, 368. (l) Pan, J. X.; Zheng, S. T.; Yang, G. Y. *Cryst. Growth Des.* **2005**, *5*, 231.

(21) Hunter, C. A.; Sanders, J, K. M. *J. Am. Chem. Soc.* **1990**, *112*, 5525.

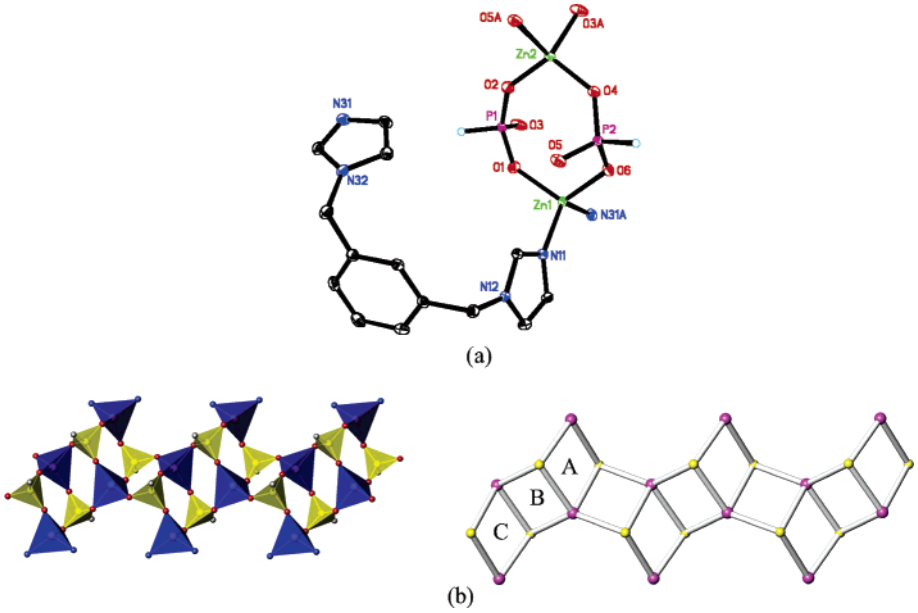


**Figure 5.** (a) ORTEP plot of the asymmetric unit of compound **5** showing the atom-labeling scheme. The ellipsoids are drawn at the 50% probability level. Three additional symmetry-related atoms are indicated by N31A, O5A, and O3A. (b) 1D inorganic framework of **5**: (left) connectivity of the $HPO_3$ (yellow) and $ZnO_2N_2/ZnO_4$ (blue) tetrahedra to the triple fused 4-rings; (right) schematic drawing of the 1D network.

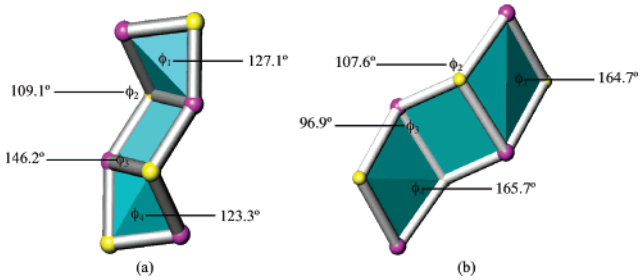


**Figure 6.** Schematic drawing of the triple fused 4-rings in **4** (a) and **5** (b) with the numbers indicating the dihedral angles between these edge-sharing planes.

**Scheme 2.** Possible Mechanism for the Formation of the One-Dimensional Chain in **5** from the Triple Fused 4-Rings in **4**

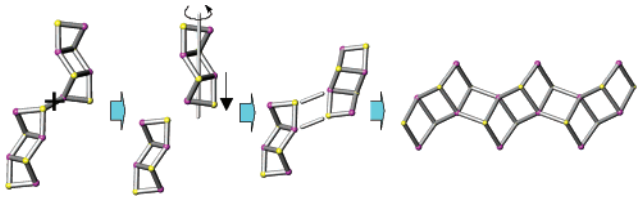

moves closer to another unit, (III) these two units are reconnected by double Zn−O−P linkages to generate a new 4-ring, and (IV) the pattern repeats to form a 1D stair step.

## Calculations

Calculations are emerging as an important tool in evaluating substructures in silicate and metal phosphate compositions.[22] Here we evaluate the relative stability of the triple 4-rings contained within the ladder structure of **1** and the stair step structure of **5**. In both cases the crystallographic coordinates were used as starting points for the calculation of the optimized geometries and relative energetics of the triple-fused 4-rings. In each case, a portion of the structure that included five fused 4-rings served as the starting point, and coordination sites that are left dangling were filled with hydroxide or imidazole groups consistent with the crystal structure. A similar procedure was not readily available for structure **4** since the triple 4-rings in this structure are connected to form 12-rings and the calculation could not be equivalently truncated. The structures of the five fused 4-rings were then optimized using quantum-mechanical methods. The PM3 semiempirical Hamiltonian,[13] as implemented in the GAMESS suite of programs,[14] was used in all calculations. The first and last rings of each chain is distorted upon minimization due to the finite size of our clusters. However, the core triple 4-rings are expected to be a genuine representation of the fused rings in the extended structures. In fact, the geometries of the optimized structures concur with the crystal structure data.

The goal of our calculations is to establish the relative strain energies of the inorganic triple 4-ring patterns alone, in the absence of ligands. Thus, although we optimized the motifs including all of the corresponding ligands and an additional ring at each side of the triple 4-ring structures, we neglect the contributions of the ligands and terminal rings in the calculation of the relative stability of the triple 4-ring structures. In this manner, we find that the triple 4-ring within the ladder structure is 17 kcal $mol^{-1}$ more stable than the triple 4-ring pattern of the stair step pattern. The minimized structures for **1** and **5** with five rings and pendant groups are shown in Figure 7. The portion of the each structure within the box is the basis for determining the relative energy of the triple 4-rings. The observation that the triple 4-ring in **1** is more stable is consistent with the common occurrence of ladders among zinc phosphates/phosphites[1a,3a,6a,f,17] and the rare occurrence of the stair step pattern observed in **5**.[4c] Although we could not estimate the relative energy of the

(22) Catlow, C. R.; Coombes, D. S.; Lewis, D. W.; Pereira, J. C. *Chem. Mater.* **1998**, *10*, 3249.

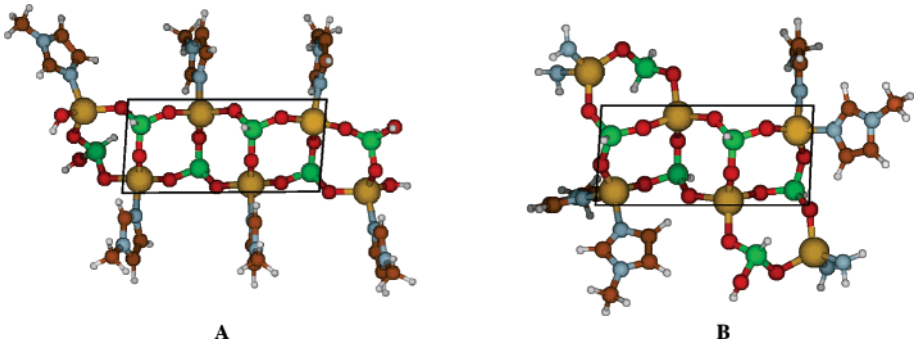


**Figure 7.** Results of the PM3 calculations shown graphically for the ladder structure, A, on the left, and the stair step structure, B, on the right. The calculated energies of the core triple 4-rings shown in the boxes establish that the triple 4-ring within ladder motif, A, is 17 kcal $mol^{-1}$ more stable than the triple 4-ring in the stair step structure, B.

triple 4-ring in **4** in a similar fashion, it is likely that it also is less stable than the ladder pattern of **1**. It is only by the presence of ligands that these distorted ring patterns can be stabilized.

## Conclusion

Five new zinc phosphites have been synthesized in the presence of 1-methylimidazole, 1-benzylimidazole, 1,4-bis-(imidazol-1-ylmethyl)benzene, and 1,3-bis(imidazol-1-yl-methyl)benzene. In compound **1**, the mono(imidazole) ligands simply decorate the ladder structure. In **2** and **3**, the zinc and phosphorus tetrahedra form $4.8^2$ inorganic sheets which are pillared in the former by C−H···$\pi$ interactions between 1-benzylimidazole ligands and by 1,4-bis(imidazol-1-ylmethyl)benzene in the latter to form similar 3D layered structures. Compounds **4** and **5** are synthesized with the same ligand, and in both structures a tertiary building united comprised of a triple fused 4-ring is identified. The triple 4-ring is also seen in the ladder structure, **1**, and has been noted previously in the literature.[4c] Calculations show that, in the absence of ligands, the triple 4-ring in the ladder structure of **1** is 17 kcal $mol^{-1}$ more stable than the triple 4-ring in **5**. Clearly the bonding requirement of the ligand plays the dominant role in determining the observed structures. This suggests that the key to hybrid materials synthesis and structure is ligand design. In each of the structures reported here it appears that the inorganic portion of the structure adopts a pattern that maximizes metal−ligand bonding and ligand−ligand interactions. Growth of the inorganic phase is modified accordingly. In consideration of structures **4** and **5**, we come to the conclusion that zinc phosphite/phosphate structures may be more predictable if rigid ligands are used to connect zinc phosphate/phosphite phases. We are currently investigating several rigid bifunctional ligands for the construction of novel inorganic/organic zinc phosphite/phosphate materials.

**Acknowledgment.** We thank R. J. Reynolds for support of this work through a McNair Postdoctoral Fellowship to J.F. We thank the NSF (Grant CHE-0131128) for funding the purchase of the Oxford Diffraction Xcalibur2 single-crystal diffractometer.

**Supporting Information Available:** Figure S1, showing the packing diagram of **1**, Figure S2, showing the helix motif in **2**, Figure S3, showing the arrangement of benzene rings in **2**, Figure S4, showing the arrangement of ligands in **3**, Figure S5, showing the arrangement of ligands in **4**, Figure S6, showing the stair-step connection mode of the 1D chain in **5**, Figure S7, showing the packing diagram of **5**, and X-ray crystallographic files in CIF format. This material is available free of charge via Internet at http://pubs.acs.org.

IC048204U